IEEE Open Journal of Vehicular Technology

Received 17 June 2024; accepted 8 July 2024. Date of publication 12 July 2024;
date of current version 26 July 2024. The review of this article was coordinated by Editor Darren Galpin.

Digital Object Identifier 10.1109/OJVT.2024.3426989

Influential Control Parameters for Autonomous Vehicles in a Mixed Environment

HOSSAM M. ABDELGHAFFAR [1,2] AND MÓNICA MENÉNDEZ [1] (Member, IEEE)

[1]Division of Engineering, New York University Abu Dhabi, Abu Dhabi 129188, UAE
[2]Department of Computer Engineering and Systems, Faculty of Engineering, Mansoura University, Mansoura 35516, Egypt

CORRESPONDING AUTHOR: HOSSAM M. ABDELGHAFFAR (e-mail: hossamvt@vt.edu).

The work of Mónica Menéndez was supported by the NYUAD Center for Interacting Urban Networks (CITIES), funded by Tamkeen under the NYUAD Research Institute Award CG001.

ABSTRACT Autonomous vehicles will be widely operated on roadways in the near future. Prior to the broad adoption of autonomous vehicles (AVs), conventional human-driven vehicles would coexist with their AVs counterparts on the same roads, resulting in traffic scenarios that had never been observed before. One such scenario involves the merging of AVs onto a main road. This study assesses the effects of incorporating AVs into a transportation system at different levels of AV penetration. This research analyzes AVs' influence by examining performance metrics such as travel time, delay, number of stops, and stop delay. The results demonstrate that introducing AVs at penetration rates of 10%, 25%, and 50% leads to an average total network delay increase of 4%, 7%, and 18%, respectively. A variety of parameters influence AV performance. To improve AV performance and, consequently, performance metrics, it is critical to identify and effectively control the influential parameters that have a significant impact on AV performance. Consequently, in this paper, we employ the quasi-optimized trajectory elementary effect sensitivity analysis approach, to identify the parameters whose variations are anticipated to significantly impact the performance metrics. The research findings reveal that the time gap, standstill distance, acceleration from a standstill, and the following distance oscillation are all influential parameters affecting the performance metrics of the network, the merging road, and the main road at various levels of AV penetration rate.

INDEX TERMS Autonomous vehicle, influential control input parameter, mixed traffic environment.

I. INTRODUCTION

The introduction of autonomous vehicles (AVs) represents a watershed moment in transportation technology, with the potential to transform our modes of commuting, travel, and goods transportation. AVs, powered by cutting-edge artificial intelligence, control mechanisms, and advanced sensor systems, and able to navigate and operate without human intervention, have triggered a seismic shift in the automotive sector [1]. Researchers, decision-makers, and the public at large have expressed a strong interest in self-driving vehicles, acknowledging their potential to enhance road safety, alleviate traffic congestion, and broaden accessibility. Nonetheless, the way to universal adoption is fraught with technical challenges, ethical quandaries, and regulatory complexities.

AV applications are diverse and expanding beyond the traditional transportation system (e.g., personal vehicles or taxis), with the potential to revolutionize a variety of industries [2], [3]. For instance, ride-sharing platforms such as Uber and Lyft have been actively experimenting with AVs in order to reduce operational costs and improve passenger accessibility [4]. Aside from personal transportation, AVs are making significant inroads into logistics and delivery services. Corporations such as Amazon and UPS are actively investigating the use of self-driving drones and delivery vans to improve the efficiency of their operations [5]. This not only boosts productivity but also has a positive impact on the environment by optimizing delivery routes. Moreover, the utilization of autonomous shuttles, modular vehicles, and buses, which also

© 2024 The Authors. This work is licensed under a Creative Commons Attribution 4.0 License. For more information, see https://creativecommons.org/licenses/by/4.0/

include first- and last-mile solutions, is being employed in the realm of public transportation [6], [7]. Furthermore, AVs are being applied to enhance healthcare transportation, serving purposes such as operating ambulances and facilitating the delivery of prescription medications [8]. As technology matures and regulations catch up, we can expect even more innovative applications in the future.

AVs have the potential to significantly enhance transportation safety, efficiency, and accessibility. However, they face several hurdles and limitations that must be overcome for their widespread adoption. For example, AVs rely on complex sensor systems, machine learning algorithms, and artificial intelligence for navigation, which makes them vulnerable to technical malfunctions. Some other challenges are described below. Cybersecurity risks: AVs are exposed to cyberattacks that can jeopardize their functionality, safety, and even privacy. Public acceptance: It remains a challenging task to persuade the general public that AVs are safe and dependable. Cost and infrastructure: The implementation of autonomous technology can be expensive, limiting access for certain groups. Moreover, infrastructure elements such as road markings and traffic signals need upgrades to accommodate AVs. In addition, there will be challenges with vehicle communication, coordination, and behavior prediction during the transition period, where autonomous and human-driven vehicles coexist on the roads. This stage necessitates special oversight, planning, and management. Therefore, it is critical to investigate the various aspects of this transformative technology, addressing both its promise as well as the challenges and questions it raises for the successful integration of AVs into the transportation ecosystem.

In accordance with research findings, AVs have the potential to alleviate traffic congestion through decreasing travel times, increasing traffic capacity, and improving safety precautions. Even with the appeal of AVs, there are several issues to consider when autonomous and human-operated vehicles (conventional vehicles, CnVs) share the same road. There will be a dynamic mix of autonomous and conventional vehicles on the road during the transitional phase preceding the widespread adoption of fully automated vehicles. Human drivers will continue to interact with other conventional vehicles as usual, but they will also need to adapt to the presence of vehicles without human operators. Furthermore, it is critical to investigate the impact of AVs coexisting with CnVs on the overall traffic performance.

Several research studies have delved into the traffic dynamics when AVs and CnVs coexist. For instance, Aleksandra et al. [9] analyzed roundabout safety levels using a VISSIM microsimulation, considering scenarios where AVs were integrated with CnVs. Their findings indicate that the introduction of AVs leads to a rise in the number of potential traffic conflicts. They investigated three types of such conflicts: accidents arising from lane change conflicts, angle accidents caused by crossing conflicts, and rear-end accidents resulting from rear-end conflicts. Their findings revealed that increasing the percentage of AVs increases the number of roundabout accidents. In addition, they stated that while most rear-end collisions are minor, they should not be overlooked when roundabout design changes occur as a result of the introduction of AVs.

Henrietta et al. [10] emphasized the potential risks and uncertainties associated with AVs operating within the framework of existing conventional traffic infrastructure. They specifically mentioned incompatibilities between current infrastructure and systems such as the speed assist system, which relies on speed limit sign recognition, as well as adaptive cruise control (ACC) and lane assist features. They also stated that an overemphasis on compliance with highly automated vehicles could be dangerous, especially if the infrastructure is not adequately adapted to accommodate them. AVs do not need to be built around existing infrastructure. Nonetheless, significant infrastructure changes are required, which may include the installation of new signs, alternative types of lanes, or even a total rebuild [11].

In a study conducted by Ramin et al. [12], they examined the anticipated effects of different levels of AVs on the safety performance of an intersection. In the first scenario, they looked at the interaction between human-driven vehicles and level 3 AVs. Their findings showed that as the presence of human-driven vehicles decreased, the average number of accidents at the intersection also decreased. In the second scenario, the study focused on the interaction between human-driven vehicles and level 5 AVs. The results indicated that when the penetration of level 5 AVs exceeded 40%, the average number of accidents decreased.

An examination of AV-involved accidents in California revealed that AVs were most often struck by CnVs because human drivers did not anticipate the AVs' behavior [12]. The process of humans adapting and learning to interact with AVs has the potential to improve intersection safety outcomes by reducing conflicts and erratic driving. Nonetheless, there is a risk that drivers will exploit AV limitations and become more aggressive in their interactions, potentially undermining the safety benefits.

Erfan et al. investigated the impact of AVs on driver behavior and traffic performance [13]. Their findings showed that CnVs drivers traveling in close proximity to a platoon of AVs with a short time headway (THW) tended to reduce their own THW and spend more time operating under a critical THW. Furthermore, driving an AV was found to reduce driver situational awareness and may contribute to increased driver fatigue, particularly in light traffic situations. They also proposed that the benefits of AVs on highways become more apparent during congested periods, such as morning or evening rush hours. They emphasized the importance of additional research into mixed-traffic scenarios involving both AVs and CnVS.

Merging onto major roads from on-ramps presents a range of potential conflicts for both automated and conventional vehicles [14]. Some of these conflicts may require immediate intervention from the driver, which can present challenges for AVs when operating in mixed-traffic environments. In

such scenarios, it's crucial to prevent AVs from encountering these conflict situations and to consider these scenarios in the controllers that are being developed to improve traffic performance. However, there is currently limited knowledge about how AVs might react in these specific situations. When AVs merge onto a main road or change lanes, they typically require a sufficient gap in the target lane. AVs equipped with lane change assistance systems may need a relatively large open space before initiating lane changes. While this is feasible and safe in smooth traffic conditions on roads without merging sections, it could pose challenges in congested traffic or with on-ramp roads. In such cases, the AV may either be unable to perform the desired maneuver or require human intervention to execute it manually [15].

The impact of differences in on-ramp merging behavior between human-driven and autonomous vehicles on traffic flow remains uncertain. Although there has been extensive research on various aspects of AVs [16], [17], [18], [19], [20], [21], to the best of our knowledge, there is currently a lack of sufficient research in this specific area. Consequently, the first objective of this research is to investigate disparities in traffic performance metrics when human-driven and autonomous vehicles merge onto major roads. This evaluation using a microscopic traffic simulation environment will consider performance measures such as travel time, delays, number of stops, and stop delays at varying levels of autonomous vehicle penetration rate. The simulations encompass two scenarios: the first scenario involves only human-driven vehicles on the network, including main and on-ramp roads. In the second scenario, AVs are introduced on both the on-ramp road and the main road, allowing an assessment of how traffic flow is affected when autonomous vehicles are integrated into the real-world transportation environment.

The performance of AVs within the simulation is impacted by a range of parameters that mimic real-world scenarios in a traffic environment, encompassing both the parameters of the car-following and the lane change models. Thus, it is crucial to identify the key parameters that have a significant influence on AV performance. As far as our knowledge extends, there has been no prior research that has delved into pinpointing the most influential parameter for AVs, to leverage this information for enhancing performance. This constitutes the second objective of our research. Sensitivity analysis (SA) can serve as a potent tool to accomplish this objective. SA refers to the investigation of how variations and uncertainties in the output of a model, whether numerical or otherwise, can be attributed to various sources of uncertainty in the model's inputs [22]. These analyses offer valuable insights into the connection between model inputs and outputs, highlighting the most influential parameters, i.e., parameters whose fluctuations are anticipated to exert substantial influences on the model's output. Nonetheless, it's important to note that several quantitative SA techniques may encounter challenges when applied to computationally intensive models such as traffic microsimulations [23]. In this paper, we employed the quasi-optimized trajectory elementary effects (QOTEE) approach as an effective and qualitative SA approach. The QOTEE approach performs exceptionally well at identifying the most influential parameters in complex models in a computationally efficient manner by computing and comparing sensitivity indices [24]. A detailed explanation of the QOTEE approach can be found in Section II. To the best of our knowledge, this research is the first attempt to identify the influential control parameters for AVs operating in a mixed-traffic environment, utilizing the microscopic traffic simulator VISSIM.

This paper aims to assess the impact of incorporating AVs on a network that includes an on-ramp road. Additionally, it introduces a practical and efficient approach designed to meet the computational complexities associated with intricate, microscopic traffic models. To summarize, the paper provides a twofold contribution: firstly, it assesses the impact of introducing AVs into the traffic system under different levels of AV penetration, focusing particularly on scenarios where AVs merge onto a major road. This assessment is based on various performance metrics such as travel time, delay, number of stops, and stop delay. Secondly, it employs a quasi-optimized trajectory elementary effects approach for the SA of AVs, involving twenty-one input parameters and generating four output measures, to identify the most influential control parameters from the input parameters associated with car following and lane change models. The output measures encompass travel time, delay, number of stops, and stop delay. The analysis is conducted at the network level, as well as for the merge road and the main road separately.

This paper is organized as follows: Section II describes the approach employed to determine the influential AV control parameters. The parameters of the car-following model used in the study are described in Section III. Section IV outlines the simulation setup, including testbed details, performance metrics, and the QOTEE input parameters. Section V presents the results of performance metrics as well as the identified influential parameters. Section VI summarises the study.

II. QOTEE APPROACH

This section introduces the quasi-optimized trajectory elementary effect (QOTEE) approach as an efficient qualitative sensitivity analysis approach based on the elementary effects (EE) method. This approach employs sensitivity indices to identify the most influential parameters in computationally expensive and/or complex models. The information disclosed by sensitivity analysis is heavily dependent on the number of simulated sample points and their location, also referred to as trajectories. Using a small number of properly distributed sample points, this section describes an effective method for identifying the most important parameters in a model with many parameters.

The EE method is an effective method for identifying the most important parameters among all those that can be embedded in a complex model [23]. Consider a model with a single output y and input X with k independent input parameters discretized into a specified number of levels (p) in the input

space φ, i.e., $\mathrm{X} = [x_1, x_2, .., x_k]$. The EE value ($ee$) of the ith input is defined for a given value of X by changing only the ith input parameter by Δ as shown in (1), where, $\Delta = p/2(p-1)$, and the relocated input point remains in φ.

$$ee_i = \frac{y(x_1, x_2, .., x_i + \Delta, .., x_k) - y(x_1, x_2, .., x_i, .., x_k)}{\Delta} \quad (1)$$

To assess the model's sensitivity, the ee must be calculated using random samples for the ith value m times across the entire input space for the k inputs [23]. Each ee associated with the ith input is calculated using two points with relative distance Δ in x_i and zero in the other coordinates. The sensitivity indices, which are the mean (μ_i), standard deviation (σ_i), and absolute mean (μ_i^*) of the m ($j = 1, 2, .., m$) random samples ees of the ith input parameter ($i = 1, 2, .., k$), can be calculated as follows:

$$\mu_i = \frac{1}{m}\sum_{j=1}^{m} ee_i^j \quad (2)$$

$$\sigma_i = \sqrt{\frac{1}{m-1}\sum_{j=1}^{m}\left(ee_i^j - \mu_i\right)^2} \quad (3)$$

$$\mu_i^* = \frac{1}{m}\sum_{j=1}^{m} |ee_i^j| \quad (4)$$

The influence of an input parameter on the output is determined by the mean (2). The standard deviation (3) quantifies the cumulative impact of the input parameter, whether it is nonlinear or interacts with other parameters. A high standard deviation indicates significant variation among the elementary effects, and this variation is highly influenced by the specific sample point at which the computation occurs, implying that the values assigned to the other parameters play a crucial role. When dealing with a model that exhibits nonmonotonic behavior or includes interaction effects, certain effects could cancel each other out during computation, resulting in a lower mean value for an influence parameter. As a result, it is more practical to use the absolute mean (4) as a more appropriate measure [25].

The values of μ and σ should be evaluated simultaneously since a parameter with elementary effects of opposing signs may have a low μ but a significant σ. Representing this graphically in the μ-σ plane enables a more precise interpretation of results, as it considers both sensitivity measures simultaneously, moreover, μ^* is an informative and concise measure [23], [26].

To identify the most influential parameters, all three statistics, μ, σ, and μ^*, should be computed. The comparison between μ and μ^*, for instance, reveals how the parameter influences the output. When both μ and μ^* have high values, this implies that the parameter not only has a significant influence on the output but also has a consistent influence in the same direction. If μ is low while μ^* is high, this indicates that the parameter in question has effects with varying signs, depending on the values of the other parameters. If μ^* is low, this indicates that the parameter is not influential. If both μ^* and σ are high, this indicates an influential parameter with non-linear effects and/or significant interactions with other parameters. If μ^* is high and σ is low, this indicates an influential parameter with linear effects and no significant interactions with other parameters.

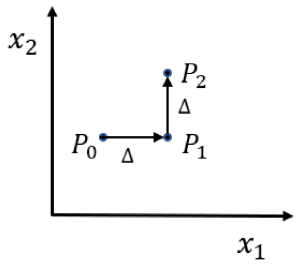

FIGURE 1. Morris trajectory for two input parameters.

Two sample points are required for each ee. Thus, to compute the sensitivity indices using m ees the simplest approach would require 2 m sample points for each input, for a total of $2mk$ model evaluations, where k represents the number of input parameters. In other words, the computational cost for the SA of such a model is $2mk$. For instance, if $m = 500$ and $k = 21$, 21000 model runs are required.

A more effective design approach that generates m trajectories, each of which consists of $(k+1)$ points in the input space was proposed by Morris [26]. This design generates m distinct ees for each input parameter, for a total of $m(k+1)$ model runs. For instance, if $m = 500$ and $k = 21$, 11000 model runs are required.

The trajectories are generated in the following manner: To begin, select a random vector X_i $(1 \times k)$ in φ. X_i is not included in the trajectory, but it serves as the basis for generating all of the trajectory points ($\mathbf{X}_{all}$, $(k+1 \times k)$ matrix). These points are derived from X_i by changing one or more of its k components by a value Δ. The idea is that two consecutive points exhibit a difference of Δ in only one component as shown in Fig. 1.

For a k-parameters model, a trajectory with $k+1$ points can provide k ees, one for each parameter. Thus, m ees can be calculated by randomly sampling m trajectories, but only with $m(k+1)$ model runs. Equation (5) shows how to construct such trajectories with the required properties, where each row in $\mathbf{X}_{all}$ represents a point on the trajectory in the input space.

$$\mathbf{X}_{all} = (\bar{\mathrm{J}}\mathrm{X}_i + (\Delta/2)[(2\mathbf{B} - \mathbf{J})\mathbf{D} + \mathbf{J}])\mathbf{P} \quad (5)$$

where $\bar{\mathrm{J}}$ is a $(k+1) \times 1$ vector of 1's, $\mathbf{B}$ is a $(k+1) \times k$ strictly lower triangle matrix of 1's, $\mathbf{J}$ is a $(k+1) \times k$ matrix of 1's. $\mathbf{D}$ is a diagonal matrix with k dimensions in which each element has an equal probability of being either +1 or -1. $\mathbf{D}$ specifies whether the parameters' values will increase or decrease along the trajectory. Meanwhile, $\mathbf{P}$ denotes a $k \times k$ random matrix with only one element in each row set to 1 and all other elements set to 0. $\mathbf{P}$ specifies the order in which the parameters are changed. $\mathbf{X}_{all}$ provides one ee for each input

parameter; the process can be repeated m times to generate m ees for each input parameter.

The aforementioned Morris trajectories are generated at random, therefore, there is a possibility that two or more of them will intersect within a specific region of the input space. Using overlapping trajectories for data sampling may result in an inaccurate and inefficient representation of the input space with a surplus of unnecessary model runs. An improvement to the sampling approach that enables more efficient exploration of the input space was proposed by Campolongo et al. [27]. Their goal was to identify an optimized trajectories (OT) subset with n trajectories with the broadest spread in the input space from a set of m trajectories to reduce the number of model executions. The term "spread" refers to the Euclidean distance between two distinct trajectories, as per (6).

$$d_{uv} = \begin{cases} \sum_{i=0}^{k} \sum_{j=0}^{k} \sqrt{\sum_{z=1}^{k} [\mathrm{X}_z^{(i)}(u) - \mathrm{X}_z^{(j)}(v)]^2} & u \neq v \\ 0 & \text{otherwise} \end{cases} \tag{6}$$

where d_{uv} is the distance between two trajectories, u and v. k is the number of input parameters, and $\mathrm{X}_z^{(i)}(u)$ represents the z coordinate of the point i on the u trajectory. The best n trajectories from m are selected by maximizing the distance d_{uv}.

After considering each possible combination of n trajectories from a set of m, the total distances between any two trajectories within each combination are computed with (7). The combination exhibiting the highest d_n value is subsequently selected. This sampling approach enhances the input space exploration, leading to a reduction in the number of model runs to $n(k+1)$. For instance, if $m = 500$, $n = 50$ and $k = 21$, 1100 model runs are required.

$$d_n = \sqrt{0.5 \left(\sum_{u=1}^{n} \sum_{v=1}^{n} d_{uv}^2 \right)} \tag{7}$$

The total number of possible combinations to find the optimized subset of n trajectories in a set of m trajectories is calculated as $m!/[n! * (m-n)!]$. This may preclude the use of OT sampling for complex models. For instance, if $m = 500$ and $n = 50$ the total number of possible combinations are 2.31×10^{69}. Although running the model is computationally feasible, checking all possible combinations to find the OT is not. An improvement to the OT sampling approach was addressed in [24]. In order to overcome such a limitation, they introduced a quasi-optimized trajectories-based elementary effect approach.

In this approach, a stepwise process is used instead of directly selecting n optimized trajectories from the initial set (S_m) of m Morris trajectories $(T_j, j = 1, 2, .., m)$. First, the distance matrix between trajectories is computed using (6), as shown in (8). The total distance between trajectories in S_m is presented in (9).

$$d_{s_m} = \begin{bmatrix} 0 & d_{T_1,T_2} & \dots & d_{T_1,T_m} \\ d_{T_2,T_1} & 0 & \dots & d_{T_2,T_m} \\ : & : & \dots & : \\ d_{T_m,T_1} & d_{T_m,T_2} & \dots & 0 \end{bmatrix} \tag{8}$$

$$d_{s_m} = \sqrt{0.5 \left(\sum_{i=1}^{m} \sum_{j=1}^{m} d_{T_i,T_j}^2 \right)} \tag{9}$$

To begin, the set S_{m-1} of $m-1$ trajectories with the greatest total distance within S_m is selected. $S_{m-1}(l)$ includes all S_m trajectories except trajectory l, i.e., $S_{m-1}(1) = \{T_2, T_3, .., T_m\}$, $S_{m-1}(2) = \{T_1, T_3, .., T_m\}$, and so on. The overall distance of the $m-1$ trajectories in the set $S_{m-1}(l)$ is calculated as shown in (10).

$$d_{s_{m-1}(l)} = \sqrt{d_{s_m}^2 - \sum_{i=1}^{m} d_{T_i,T_l}^2} \tag{10}$$

Then, the set (S_{m-2}) of $m-2$ trajectories with the greatest dispersion is chosen in the second step based on S_{m-1}. This process is repeated until only n trajectories remain in the set, giving rise to the quasi-optimized trajectories. The number of trajectories in the optimal set is reduced by one at each step. While the trajectories from the QOTEE and OT approaches may not be identical, validation experiments in [24], [25], [28] show their significant similarity and the QOTEE's ability to improve input space coverage over the regular Morris trajectories. To obtain the final optimal set, this approach considers $(m-n+1) * (m+n)/2$ combinations. For instance, if $m = 500$ and $n = 50$ the total number of possible combinations is 18875 rather than 2.31×10^{69} for the OT approach.

III. CAR FOLLOWING MODEL

This section presents an overview of the Wiedemann-99 (W-99) car-following model. The W-99 model, a psychophysical model, employs thresholds or action points at which the drivers' behavior changes [29], [30]. The stimulus that causes the following vehicle to react, according to Wiedemann, is based on the relative speed of the leading and following vehicles. There are four distinct driving regimes proposed, each with a distinct perception threshold.

- Free flow regime: the subject vehicle is not impacted by a leader; the driver attempts to maintain a desired speed while employing a speed-dependent maximum acceleration to achieve that speed.
- Closing regime: the driver observes a slower vehicle ahead and gradually decreases his/her speed until it aligns with the speed of the leading vehicle. This action effectively reduces the relative speed to zero while maintaining the desired gap. Subsequently, the driver transits into the following regime.
- Following regime: the follower driver naturally follows the leading vehicle, aiming to sustain an optimal gap and achieve a relative speed of zero through relatively gentle accelerations or decelerations.

TABLE 1 W-99 Model Parameters

Parameter	unit	Description
$CC0$	m	Standstill distance, the desired gap between two stopped vehicles.
$CC1$	s	Time gap, the time gap maintained by the following driver to ensure safety while in motion.
$CC2$	m	Following distance oscillation, the maximum allowable distance a driver permits beyond the safe following distance from the vehicle ahead before moving up consciously.
$CC3$	s	Perception threshold for consequences, the time it takes to reach the (unbraked) safe following distance to a slower vehicle ahead when the deceleration process begins.
$CC4$	m/s	Negative speed difference, the minimum relative speed to the vehicle ahead while in the following regime.
$CC5$	m/s	Positive speed difference, the maximum relative speed to the vehicle ahead while in the following regime.
$CC6$	1/(m.s)	Influence of distance on oscillation, the impact of distance on speed oscillation during the following regime
$CC7$	m/s^2	Acceleration during oscillation, acceleration oscillation during the following regime.
$CC8$	m/s^2	Acceleration from a standstill, acceleration from a complete stop is constrained by the vehicle type's desired and maximum acceleration functions.
$CC9$	m/s^2	Acceleration at 80 km/h, acceleration at 80 km/h is constrained by the vehicle type's desired and maximum acceleration curves.

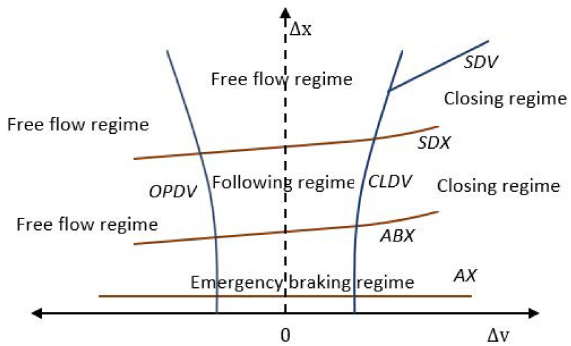

FIGURE 2. Driving regimes.

- Emergency braking regime: when the gap between the vehicles tumbles below a critical limit, the driver of the trailing vehicle responds by applying the vehicle's maximum braking power to avoid a collision.

The parameters of the W-99 car-following model denoted as $CC0 - CC9$ in Table 1, play a crucial role in determining six distinct perceptual thresholds or boundaries of these regimes. Specifically, the first seven parameters ($CC0 - CC6$) are employed in the computation of the thresholds for car-following, whereas the remaining parameters have various other functions [31], [32].

The thresholds for classifying the regimes are defined below, also, shown in Fig. 2, whereas (11)–(16) outline the relationships between W-99 parameters and the corresponding thresholds.

- AX [m]: desired gap between two standing vehicles.
- ABX [m]: desired minimum safe following gap.
- SDX [m]: maximum following gap in the following regime.
- SDV [m/s]: points at long distances at which a driver realizes that he is approaching a slower preceding vehicle.
- $CLDV$ [m/s]: acronym for closing delta velocity at short distances, which occurs when drivers perceive their speeds to be greater than the speed of the preceding vehicle, taking into account additional deceleration by applying the brakes over short decreasing distances.
- $OPDV$ [m/s]: short-distance points at which drivers realize they are traveling at a slower speed than the vehicle ahead of them and thus begin to accelerate.

$$AX = CC0 \tag{11}$$

$$ABX = AX + CC1.v_s \tag{12}$$

$$v_s = \begin{cases} v_f & \Delta v < 0 \\ v_p + \Delta v.\text{rand}[-0.5, 0.5] & \text{otherwise} \end{cases}$$

$$SDX = ABX + CC2 \tag{13}$$

$$SDV = -CC4 - \frac{\Delta x - SDX}{CC3} \tag{14}$$

$$CLDV = \begin{cases} -CC4 + CC6 \times (\Delta x - L_p)^2 & v_p > 0 \\ 0 & \text{otherwise} \end{cases} \tag{15}$$

$$OPDV = \begin{cases} -CC5 - CC6 \times (\Delta x - L_p)^2 & v_f > CC5 \\ -CC6 \times (\Delta x - L_p)^2 & \text{otherwise} \end{cases} \tag{16}$$

where v_p is the speed of the preceding vehicle, v_f is the speed of the following vehicle, and Δv is the relative speed between the follower and the preceding vehicle. When the following vehicle is slower than the preceding vehicle, v_s equals v_f. Otherwise, v_s is equal to v_p plus a random error, calculated by multiplying Δv by a random value within the range of -0.5 to 0.5. v_s is used to determine the safe distance maintained by the following driver to ensure safety while in motion. Δx is the relative spacing between the follower and the preceding vehicle, and L_p is the length of the preceding vehicle [32].

IV. EXPERIMENTAL SETUP

This section describes the testbed (section IV-A) and the performance metrics (section IV-B) that were used to evaluate the system's performance, as well as the input parameters for the proposed QOTEE approach (section IV-C).

A. TESTBED

The simulation utilized a 1000-meter stretch of road with two straight lanes and a 420-meter-long on-ramp that imitates a real-world road segment, as shown in Fig. 3. The road had no vehicles at the beginning of the simulation, and the simulation lasted one hour. Additional time was allocated for network clearance, as well as a five-minute warm-up period. The simulation operated with a time step of 0.1 seconds.

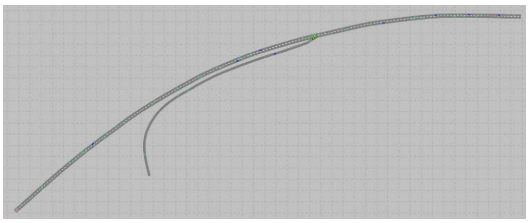

FIGURE 3. Network, VISSIM software.

There are two types of vehicles: autonomous vehicles (AVs) and conventional vehicles (CnVs). In PTV VISSIM, AVs and CnVs are simulated using the same behavioral models such as, Wiedemann's 99 car following model [33] and Sparmann's lane changing model [34]. These models govern vehicle acceleration, deceleration, following, and lane changing to simulate realistic traffic scenarios. By adjusting parameters for each vehicle type (AV or CnV) within the simulation [35], [36], PTV VISSIM differentiates their behavior without using separate equations, ensuring realistic and efficient simulations. PTV VISSIM, developed by the PTV Group, is a sophisticated microscopic traffic simulation software that is widely used to analyze and replicate traffic dynamics in a variety of environments, including urban roads, highways, intersections, and public transit networks. Its capabilities enable researchers to meticulously model vehicles, pedestrians, and other relevant traffic components while observing their interactions in a simulated environment. This tool enables researchers to evaluate the effectiveness of transport systems and investigate various traffic management strategies [35]. AVs use advanced technologies to operate and maneuver without human intervention. These technologies typically include a diverse set of sensors such as radar, lidar, cameras, and ultrasonic sensors, as well as sophisticated control systems and algorithms for perception, decision-making, and management. AVs have the potential to transform transport by enhancing safety, efficiency, and accessibility. They interact with each other and infrastructure components, enabling synchronized movement and optimized traffic flow [36]. CnVs on the other hand, are human-driven vehicles without autonomous features. These vehicles are entirely dependent on human drivers for operation, navigation, and decision-making while on the road. Unlike AVs, CnVs lack sophisticated sensing, computing, and control systems. The main road demand was set at 1000 vehicles per hour per lane, and the on-ramp demand was set at 300 vehicles per hour per lane at a speed of 50 kilometers per hour. These demands depict traffic conditions that are relatively uncongested and are suitable for assessing the performance of AVs. This is because AVs might not encounter challenges in low-traffic situations, and there would be no discernible distinction in performance between AVs and CnVs under high-congestion circumstances. The percentage of AVs on the main and on-ramp roads varies between 10% and 50%. For comparison, we consider a base case scenario in which the simulation runs with only CnVS in the scene.

B. PERFORMANCE METRICS

The simulations encompassed two scenarios: in the first, or "base" scenario, only CnVs with human drivers were used on both the main and on-ramp roads. The second scenario, known as the "mixed" scenario, involved the introduction of AVs at various penetration rates onto the on-ramp and main roads in order to investigate the AVs' performance when merging onto the main road as well as their impact on the measures of effectiveness (MOE).

Multiple performance metrics were calculated, namely, average travel time (ATT), average total delay (ATD), average number of stops (ANS), and average stop delay (ASD). The percentage change in each measure of effectiveness (MOEPC, %) was computed to illustrate the disparities in performance metrics between the two scenarios. Equation (17) is used to represent the MOEPC. The MOEs are defined further below.

- ATT: average travel time to traverse a road or network, expressed in seconds.
- ATD: average travel delay, calculated in seconds by subtracting the theoretical travel time from the actual travel time. The theoretical travel time is calculated in the absence of other vehicles or reasons to stop.
- ANS: average number of stops, determined by dividing the overall number of stops by the overall number of simulated vehicles.
- ASD: average stopped duration for all simulated vehicles in seconds.

$$\text{MOEPC} = \frac{\text{MOE(mixed)} - \text{MOE(base)}}{\text{MOE(base)}} \times 100 \qquad (17)$$

C. QOTEE INPUT PARAMETERS

This section presents the application of the proposed QOTEE approach with the case study on the network shown in Section IV-A. VISSIM encompasses a wide range of input parameters that can change depending on the software version, installed modules, and user preferences. For example, version 5.40 has approximately 192 parameters [24]. VISSIM parameters encompass various aspects, including road infrastructure, which is critical in modeling both physical and stationary network elements such as links, connectors, detectors, parking lots, and signposts. Once the physical layout of the modeling system has been determined, specifying the vehicle characteristics that use the infrastructure becomes critical. This includes describing parameters like traffic volume, vehicle types, and route choices. Furthermore, it is critical to define traffic control methods for managing conflicting and prioritized movements, which can be accomplished through un-signalized or signalized traffic signal control.

To identify the most influential parameters that affect AVs' performance, a preliminary, extensive literature review was conducted to generate a possible list of critical parameters, reducing the number of parameters to be evaluated with the SA. Since our research focuses on AV behavior and the parameters that influence it, a vehicle's behavior in VISSIM is determined

TABLE 2 QOTEE Input Parameters

Parameter	Description & values			
	Description	Default	Min	Max
CFM				
x1	$CC0$; Standstill distance [m]	1.5	1	3
x2	$CC1$; time gap [s]	1.5	0.6	1.5
x3	$CC2$; following distance oscillation [m]	0	0	4
x4	$CC3$; perception threshold for consequences [s]	−10	−14	−6
x5	$CC4$; negative speed difference [m/s]	−0.1	−0.3	0
x6	$CC5$; positive speed difference [m/s]	0.1	0	0.3
x7	$CC6$; influence of distance on oscillation [1/(m.s)]	0	0	11
x8	$CC7$; acceleration during oscillation[m/s^2]	0.1	0.05	0.3
x9	$CC8$; acceleration from a standstill [m/s^2]	3.0	1.5	5
x10	$CC9$; acceleration at 80 km/h [m/s^2]	1.2	0.5	2.5
LCM				
x11	maximum deceleration (own) [m/s^2]	−3.5	−6	−2
x12	-1 m/s2 per distance (own) [m]	80	50	150
x13	accepted deceleration (own) [m/s^2]	−1	−1.5	−0.5
x14	maximum deceleration (trail) [m/s^2]	−2.5	−5	−1
x15	-1 m/s2 per distance (trail) [m]	80	50	150
x16	accepted deceleration (trail) [m/s^2]	−1	−1.5	−0.5
x17	minimum clearance (front/rear) [m]	0.5	0.3	1.0
x18	safety distance reduction factor [-]	1	0	1
x19	maximum deceleration for cooperative braking [m/s^2]	−2.5	−5	−1
x20	emergency stop distance [m]	5	5	10
x21	lane change distance [m]	200	150	250

by its type and the driving behavior parameter set assigned to the link that the vehicle is currently on. The vehicle type determines the vehicle's mechanical characteristics, which include width, length, maximum acceleration and deceleration, and is also associated with the drivers' desired acceleration and deceleration. The driving behavior parameter set includes numerous parameters that govern various types of behavior such as car following, lane change, lateral behavior, and signal control behavior. Among these driving behavior parameters, we believe that the performance of AVs within the on-ramp merging application is mostly impacted by parameters associated with the car-following and lane change models.

Table 2 displays the 21 parameters that were chosen as the candidate influential parameters, comprising ten parameters for the W-99 car following model (CFM) and eleven for the lane change model (LCM). These specific parameters were utilized as input parameters for the QOTEE approach. The CFM parameters, denoted as x1-x10 in Table 2, are explained in Section III, whereas the LCM parameters, denoted as x11-x21 in Table 2, are explained below. Table 2 displays the default values for the AVs parameters following the PTV VISSIM [35] and the parameter bounds used within the approach.

The maximum deceleration parameters (x11 and x14) refer to the highest possible rate of slowing down when transitioning between lanes, taking into account the prescribed routes for overtaking with the lane-changing vehicle and the behavior of the vehicle behind, in the destination lane. The deceleration change parameters (x12 and x15) linearly reduce the maximum deceleration to the accepted deceleration with increasing distance from the emergency stop distance. The accepted deceleration parameters (x13 and x16) are the minimum deceleration for the lane changing and the trailing vehicles during a lane change, respectively. The minimum clearance (x17) refers to the smallest gap required between two vehicles for a lane change to take place. When making a lane change in regular traffic conditions, it might be necessary to have a larger minimum distance between vehicles to adhere to speed-dependent safety guidelines. In the process of changing lanes, VISSIM calculates the reduced safety distance by multiplying the initial safety distance by a factor known as the safety distance reduction factor (x18). The cooperative braking's maximum deceleration (x19) determines how much the trailing vehicle collaboratively applies its brakes to facilitate a potentially leading vehicle's lane change into its lane. The emergency stop distance (x20) is applied to simulate how vehicles adhering to their designated route or those with dynamically assigned paths follow the lane change protocol. When these vehicles are unable to reach their intended lanes before reaching a connector at the emergency stop position, they will stop and remain stationary until a suitably sizable gap becomes available. The lane change distance (x21) indicates a point before a connector where vehicles on routes or paths leading through this connector engage in lane changes and strive to choose a lane that permits them to access the connector without changing lanes.

During the simulations, four different model outputs from the main road, the on-ramp road, and the entire network were collected and utilized for the sensitivity analysis. Specifically, travel time, delay, number of stops, and stop delay. These outputs represent the average results obtained by running the model with different random seeds. In the context of the QOTEE approach, 50 trajectories ($n = 50$) were selected from a pool of 500 Morris trajectories ($m = 500$). As described in Section II, a total of 1100 model runs were necessary, each employing a distinct set of 21 input parameters. As previously stated, we calculated the average output for each of these 1100 runs across five random seeds, resulting in a total of 5500 runs for each set of simulations.

V. SIMULATION RESULTS

This section investigates the performance of AVs during the merging process onto the main road and examines how this performance impacts effectiveness measures at various AV penetration rates (AVPR), Section V-A. Additionally, it reveals the most influential parameters impacting AVs' performance in Section V-B.

A. PERFORMANCE MEASURES

Tables 3 to 5 display the MOEPC for the entire network, the on-ramp road, and the main road, respectively across a range

TABLE 3 MOEPC (%) network results

AVPR(%)	MOE			
	ATT	ATD	ANS	ASD
10	0.14	3.73	18.47	7.81
25	0.27	6.90	31.25	9.18
50	0.70	18.31	75.47	36.52

TABLE 4 MOEPC (%) on-ramp road results

AVPR(%)	MOE			
	ATT	ATD	ANS	ASD
10	1.08	5.50	18.58	7.74
25	1.25	6.39	31.85	9.26
50	4.68	23.86	76.27	37.02

TABLE 5 MOEPC (%) main road results

AVPR(%)	MOE			
	ATT	ATD	ANS	ASD
10	0.07	2.82	99.9	322.34
25	0.19	7.68	100.00	100.00
50	0.40	15.66	99.36	244.47

of performance metrics. These were obtained employing ten various random seeds and varying AV penetration rates.

These findings reveal that introducing AVs into the network leads to a deterioration in the performance measures for the merging road, the main road, and the entire network when compared to the baseline scenario featuring solely conventional human-driven vehicles. Furthermore, increasing the AVPR has the effect of increasing (worsening) the average travel time, the average delay, the average number of stops, and the average stop delay when compared to the base scenario. This may stem from the autonomous vehicle's cautious maneuvers designed to prevent accidents and ensure safety. Although the MOEPC values for ANS and ASD in Table 5 are approaching or suppressing 100 percent, it's worth noting that their MOE values are almost zero. Consequently, these MOEPCs can be considered unchanged for the main road, with the merging road being the cause of network MOEPCs. Consequently, it is crucial to develop an improved control strategy for the AVs to facilitate smooth merging without compromising network performance. To achieve this, an SA is performed to identify the most influential parameter that, when controlled, can improve performance metrics.

B. INFLUENTIAL PARAMETERS

In this section, we unveil the parameters that exert the most significant influence on travel time, delay, number of stops, and stop delay at various penetration rates, specifically at

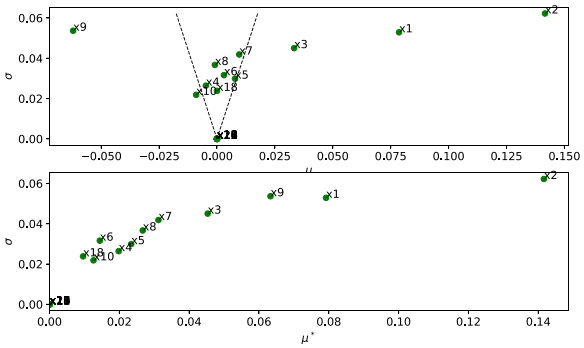

(a) Network

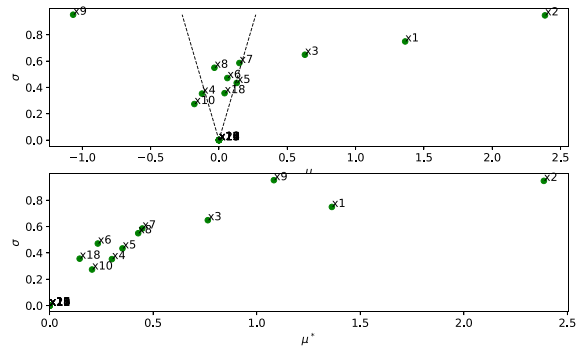

(b) Merge road

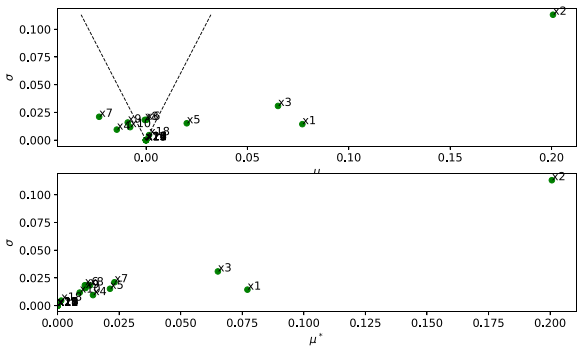

(c) Main road

FIGURE 4. QOTEE average *travel time* results at 50% AVPR.

50%, 25%, and 10%. In accordance with the QOTEE approach, the 21 input parameters were assigned values that fell within the specified ranges, as detailed in Table 2. We conducted simulations for the 50 optimized trajectories, achieving broader coverage of the sampling input space. Then, the average output results of five different random seeds and the sensitivity indices (i.e., μ, σ, and μ^*) were computed to identify the influential parameters.

Figs. 4–7 illustrate the outcomes of the sensitivity indices (SI) at a 50% AV penetration rate (AVPR) for the four performance measures concerning the entire network, the merging

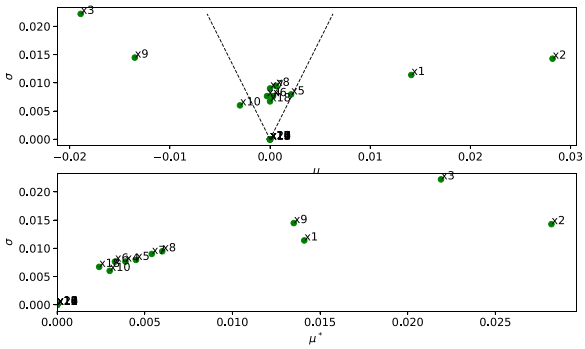

(a) Network

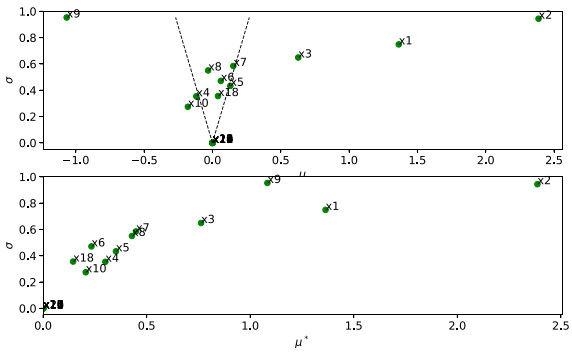

(b) Merge road

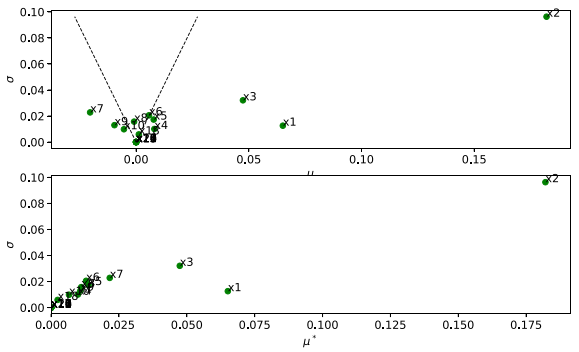

(c) Main road

FIGURE 5. QOTEE average *total delay* results at 50% AVPR.

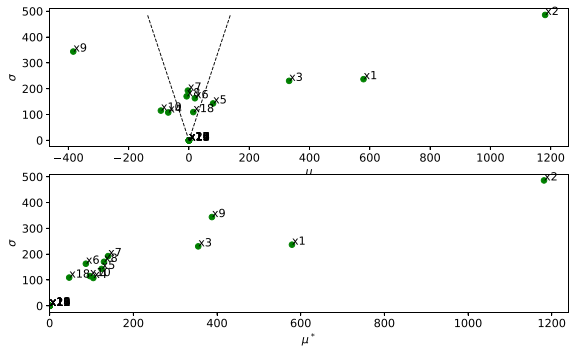

(a) Network

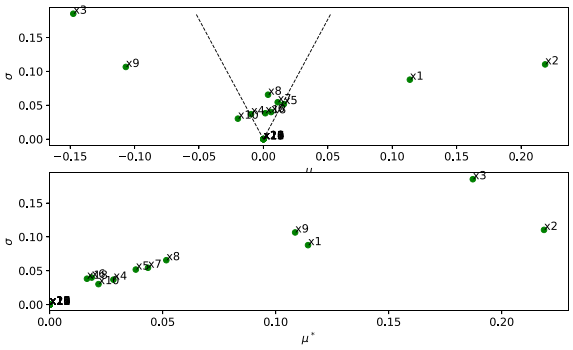

(b) Merge road

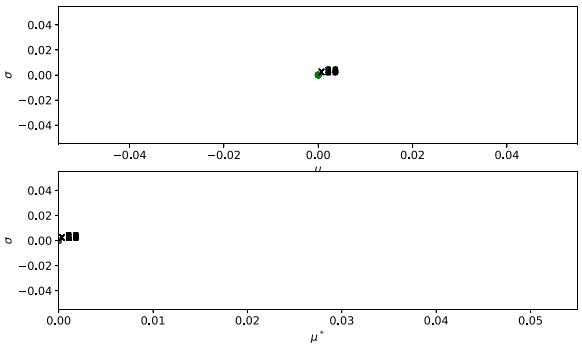

(c) Main road

FIGURE 6. QOTEE average *number of stops* results at 50% AVPR.

road, and the main road. When analyzing sensitivity indices results, it is critical to focus on relative differences rather than numerical values. To the best of our knowledge, there is no quantitative method for interpreting the results other than qualitatively comparing the SI of various parameters.

According to the results shown in Figs. 4–7, it is clear that the time gap parameter (x2) has the most influence, as evidenced by the highest values for μ^* for the four performance measures across the entire network, as well as the merge and the main roads. Additionally, x2 exhibits the highest σ value in all cases, except for the average number of stops on the merge road, where it has the second-highest value. This suggests that variations in x2 can lead to significant nonlinear effects and/or interactions with the other parameters. To evaluate the sensitivity of all the other parameters, we plotted in the (μ-σ) plot a wedge defined by two lines corresponding to μ=±2 times the standard error of the mean, where the standard error of the mean is calculated as the standard deviation (σ) divided by the square root of the sample size ($n = 50$) [37]. Any parameter outside the wedge is expected to influence the model output. Consequently, parameters x1 and x3 can also be considered influential parameters, although their variations have a smaller impact on the model output and are less correlated with other parameters (lower σ) compared to parameter x2. Moreover, the parameter x9 has a low μ but a high μ^* and σ. This implies that this parameter has both positive and negative effects. As a result, it is reasonable to consider x9 as an influential parameter too. In light of these

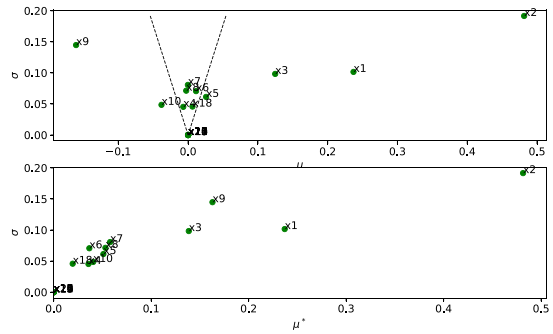

(a) Network

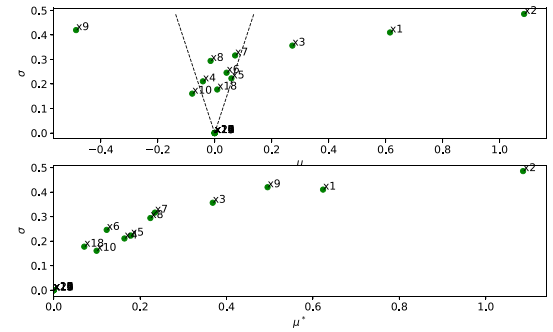

(b) Merge road

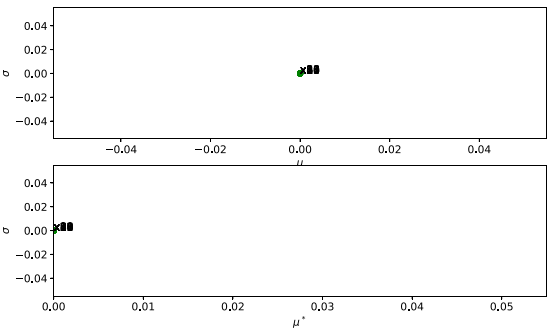

(c) Main road

FIGURE 7. QOTEE average *stop delay* results at 50% AVPR.

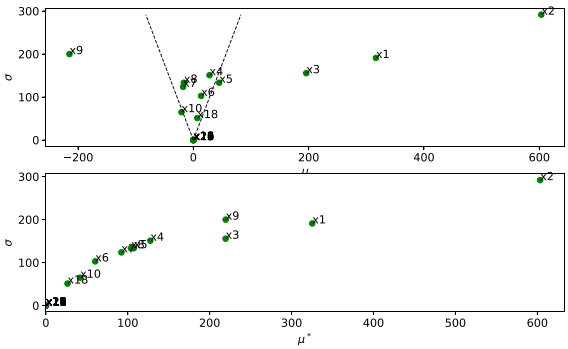

(a) Average travel time

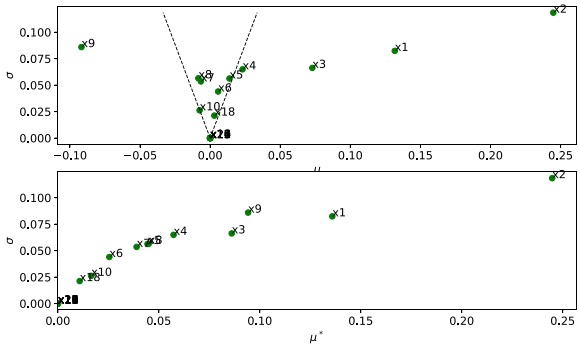

(b) Average total delay

FIGURE 8. QOTEE network results at 25% AVPR.

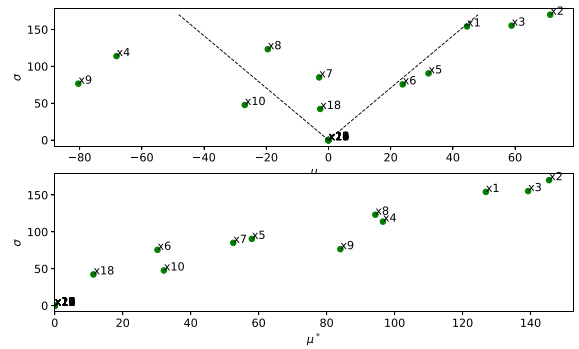

(a) Average travel time

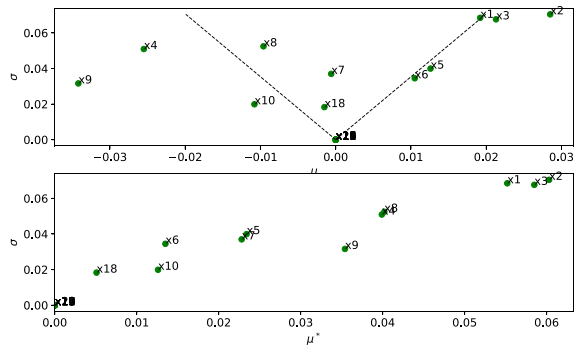

(b) Average total delay

FIGURE 9. QOTEE network results at 10% AVPR.

results, the parameters x2, x1, x3, and x9 can be regarded as influential, with x2 standing out as the most influential among them.

Furthermore, this study investigated the significant parameters influencing performance metrics at 25% and 10% AVPR. Figs. 8 and 9 show the sensitivity indices for the average travel time and average delay of the entire network. These findings show that the time gap parameter, denoted as x2, has the highest μ, μ^* and σ values, implying that it is the most influential parameter.

The findings reveal that the distance between stationary vehicles and the acceleration from a complete stop are influential parameters. Furthermore, they reveal that the following gap between moving vehicles is also influential, represented by the time gap and the following distance oscillation, with the time gap being the most influential parameter.

In this study, we evaluated the proposed approach on a road segment, representative of sections between traffic signals or short arterial or highway segments. To maximize the available space for data collection and analysis, we opted not to include a lead-in area, mirroring the absence of such areas in many real-world scenarios. Despite implementing a warmup period, this approach may not adequately stabilize vehicle behavior post-warmup, especially in terms of lane distribution and platoon formation. Therefore, future studies should consider incorporating a lead-in area when applicable and conducting tests on a broader network to boost the generalizability of the findings presented here.

The interaction between human-driven and autonomous vehicles influences the traffic environment. Therefore, to improve AV performance and, consequently, performance metrics, it is critical to identify the influential parameters that have a significant impact on AV performance. Subsequently, it is essential to develop a control strategy to regulate these parameters to dynamic environmental changes, along with a cooperative algorithm for human-driven vehicles [19], all geared towards improving network performance.

VI. CONCLUSION

The widespread deployment of autonomous vehicles (AVs) on public roads is expected shortly. However, before AVs achieve widespread adoption, traditional human-driven vehicles will coexist with them, ushering in entirely new traffic scenarios. One notable scenario is the merging of AVs onto major roads. In this paper, we modeled and evaluated the impact of introducing AVs at various penetration rates on the performance of a network featuring an on-ramp. This evaluation included a comparison of several performance metrics, i.e., total delay, travel time, stop delay, and number of stops, to a baseline scenario with only conventional vehicles present. The results indicated that introducing AVs at penetration rates of 10%, 25%, and 50% led to an average total network delay increase of 4%, 7%, and 18%, respectively. Furthermore, it was observed that at penetration rates of 10%, 25%, and 50%, there was an average total on-ramp delay increase of 5.5%, 6.4%, and 24%, respectively. It was also found that at penetration rates of 10%, 25%, and 50%, there was an average stop network delay increase of 8%, 9.2%, and 37%, respectively. In summary, raising the AV penetration rate had a detrimental effect on all performance metrics for the network, the main road, and the merge road. This could be attributed to AVs' cautious operations to ensure safety.

The performance of AVs is influenced by a variety of parameters, including those in the car-following and lane-change models. As a result, it is critical to identify and regulate the influential parameters that impact AV performance, thereby enhancing performance metrics. Hence, we employed the quasi-optimized trajectory elementary effects approach, which efficiently identifies the most influential input parameters within complex microscopic traffic models through the computation and comparison of sensitivity indices. The results reveal that the time gap, standstill distance, acceleration from a standstill, and following distance oscillation are all influential parameters. Among these, the time gap, associated with the car-following model, stands out as the most influential input parameter impacting the performance metrics of the network, merge road, and main road under various levels of AV penetration rates.

This research offers valuable insights into the impact of introducing AVs into the traffic environment on traffic mobility. It also highlights the influential control parameters impacting AV performance, aiming to enhance their performance. In light of the findings gained from this research, future research will be dedicated to developing a control strategy for regulating the influential parameters to enhance the performance of AVs and, consequently, the overall network performance.

REFERENCES

[1] F. Francesca, N. Nader, S. O. Eurich, M. Tripp, and N. Varadaraju, "Examining accident reports involving autonomous vehicles in California," vol. 12, no. 9, Sep. 2017, Art. no. e0184952, doi: 10.1371/journal.pone.0184952.

[2] S. A. Cohen and D. Hopkins, "Autonomous vehicles and the future of urban tourism," *Ann. Tourism Res.*, vol. 74, pp. 33–42, 2019.

[3] M. N. Ahangar, Q. Z. Ahmed, F. A. Khan, and M. Hafeez, "A survey of autonomous vehicles: Enabling communication technologies and challenges," *Sensors*, vol. 21, no. 3, 2021, Art. no. 706. [Online]. Available: https://www.mdpi.com/1424-8220/21/3/706

[4] B. Schaller, "The new automobility: Lyft, uber and the future of american cities," Transportation Research Board Annual Meeting, Tech. Rep., 2018. [Online]. Available: http://www.schallerconsult.com/rideservices/automobility.pdf

[5] M. Roca-Riu and M. Menendez, "Logistic deliveries with drones: State of the art of practice and research," in *Proc. 19th Swiss Transport Res. Conf.*, 2019.

[6] Z. Khan and M. Menendez, "Application of modular vehicle technology to mitigate bus bunching," *Transp. Res. Part C: Emerg. Technol.*, vol. 146, 2023, Art. no. 103953. [Online]. Available: https://www.sciencedirect.com/science/article/pii/S0968090X22003667

[7] Z. Khan and M. Menendez, "Bus splitting and bus holding: A new strategy using autonomous modular buses for preventing bus bunching," *Transp. Res. Part A: Policy Pract.*, vol. 177, 2023, Art. no. 103825.

[8] G. J. Hannoun and M. Menéndez, "Modular vehicle technology for emergency medical services," *Transp. Res. Part C: Emerg. Technol.*, vol. 140, 2022, Art. no. 103694. [Online]. Available: https://www.sciencedirect.com/science/article/pii/S0968090X22001358

[9] A. D. Tibljaš, T. Giuffrè, S. Surdonja, and S. Trubia, "Introduction of autonomous vehicles: Roundabouts design and safety performance evaluation," *Sustainability*, vol. 10, no. 4, 2018, Art. no. 1060. [Online]. Available: https://www.mdpi.com/2071-1050/10/4/1060

[10] H. Lengyel, T. Tettamanti, and Z. Szalay, "Conflicts of automated driving with conventional traffic infrastructure," *IEEE Access*, vol. 8, pp. 163280–163297, 2020, doi: 10.1109/ACCESS.2020.3020653.

[11] H. Liu et al., "Urban infrastructure design principles for connected and autonomous vehicles: A case study of oxford, UK," *Comput. Urban Sci.*, vol. 3, no. 1, 2023, Art. no. 34.

[12] R. Arvin, M. Kamrani, A. J. Khattak, and J. R. Torres, "Safety impacts of automated vehicles in mixed traffic," in *Proc. Transp. Res. Board 97th Annu. Meeting*, Washington, DC, USA, Jan. 2018. [Online]. Available: https://trid.trb.org/view/1494288

[13] E. Aria, J. Olstam, and C. Schwietering, "Investigation of automated vehicle effects on driver's behavior and traffic performance," *Transp. Res. Procedia*, vol. 15, pp. 761–770, 2016, doi: 10.1016/j.trpro.2016.06.063.

[14] A. M. Soekroella, B. V. Arem, I. R. Wilmink, and S. C. Calvert, "Considering knowledge gaps for automated driving in conventional traffic," in *Proc. 4th Int. Conf. Adv. Civil, Struct. Environ. Eng.*, Rome, Italy, Dec. 2016, pp. 102–111, doi: 10.15224/978-1-63248-114-6-33.

[15] S. C. Calvert, W. J. Schakel, and J. W. C. van Lint, "Will automated vehicles negatively impact traffic flow?," *J. Adv. Transp.*, vol. 2017, pp. 1–17, 2017, doi: 10.1155/2017/3082781.

[16] S. A. Bagloee, M. Tavana, M. Asadi, and T. Oliver, "Autonomous vehicles: Challenges, opportunities, and future implications for transportation policies," *J. Modern Transp.*, vol. 24, no. 4, pp. 284–303, Aug. 2016, doi: 10.1007/s40534-016-0117-3.
[17] S. I. Guler, M. Menendez, and L. Meier, "Using connected vehicle technology to improve the efficiency of intersections," *Transp. Res. Part C: Emerg. Technol.*, vol. 46, pp. 121–131, 2014. [Online]. Available: https://www.sciencedirect.com/science/article/pii/S0968090X14001211
[18] L. Mora, X. Wu, and A. Panori, "Mind the gap: Developments in autonomous driving research and the sustainability challenge," *J. Cleaner Prod.*, vol. 275, Dec. 2020, Art. no. 124087, doi: 10.1016/j.jclepro.2020.124087.
[19] H. M. Abdelghaffar, M. Chaqfeh, N. Fejzic, T. Rahwan, Y. Zaki, and M. Menendez, "Leveraging autonomous vehicles to tally cooperative driving behavior," *IEEE Access*, vol. 11, pp. 25455–25466, 2023, doi: 10.1109/ACCESS.2022.3231134.
[20] D. Elliott, W. Keen, and L. Miao, "Recent advances in connected and automated vehicles," *J. Traffic Transp. Eng. (English Edition)*, vol. 6, no. 2, pp. 109–131, Apr. 2019, doi: 10.1016/j.jtte.2018.09.005.
[21] K. Yang, S. I. Guler, and M. Menendez, "Isolated intersection control for various levels of vehicle technology: Conventional, connected, and automated vehicles," *Transp. Res. Part C: Emerg. Technol.*, vol. 72, pp. 109–129, 2016.
[22] F. Campolongo, S. Tarantola, A. Saltelli, and M. Ratto, *Sensitivity Analysis in Practice: A Guide to Assessing Scientific Models*. New York, NY, USA: Wiley, 2004.
[23] A. Saltelli et al., *Global Sensitivity Analysis: The Primer*. New York, NY, USA: Wiley, 2008.
[24] Q. Ge and M. Menendez, "An efficient sensitivity analysis approach for computationally expensive microscopic traffic simulation models," *Int. J. Transp.*, vol. 2, no. 2, pp. 49–64, 2014.
[25] Q. Ge, B. Ciuffo, and M. Menendez, "An exploratory study of two efficient approaches for the sensitivity analysis of computationally expensive traffic simulation models," *IEEE Trans. Intell. Transp. Syst.*, vol. 15, no. 3, pp. 1288–1297, Jun. 2014.
[26] M. D. Morris, "Factorial sampling plans for preliminary computational experiments," *Technometrics*, vol. 33, no. 2, pp. 161–174, 1991.
[27] F. Campolongo, J. Cariboni, and A. Saltelli, "An effective screening design for sensitivity analysis of large models," *Environ. Modelling Softw.*, vol. 22, no. 10, pp. 1509–1518, 2007.
[28] Q. Ge, B. Ciuffo, and M. Menendez, "Comprehensive approach for the sensitivity analysis of high-dimensional and computationally expensive traffic simulation models," *Transp. Res. Rec.*, vol. 2422, no. 1, pp. 121–130, 2014.
[29] M. Zhu et al., "Modeling car-following behavior on urban expressways in shanghai: A naturalistic driving study," *Transp. Res. Part C: Emerg. Technol.*, vol. 93, pp. 425–445, 2018.
[30] A. A. Chaudhari, K.K. Srinivasan, B. Rama Chilukuri, M. Treiber, and O. Okhrin, "Calibrating wiedemann-99 model parameters to trajectory data of mixed vehicular traffic," *Transp. Res. Rec.*, vol. 2676, no. 1, pp. 718–735, 2022.
[31] Z. Shen, X. Zhang, S. Wang, and D. Yang, "A car following based rate control algorithm for vanet in intelligent transportation systems," in *Proc. IEEE Wireless Commun. Netw. Conf.*, 2018, pp. 1–6.
[32] K. Aghabayk, M. Sarvi, W. Young, and L. Kautzsch, "A novel methodology for evolutionary calibration of vissim by multi-threading," *Australas. Transport Res. Forum*, vol. 36, no. 1, 2013, pp. 1–15.
[33] V. Zeidler, H. S. Buck, L. Kautzsch, P. Vortisch, and C. M. Weyland, "Simulation of autonomous vehicles based on Wiedemann's car following model in PTV vissim," in *Proc. 98th Annu. Meeting Transp. Res. Board*, Washington, DC, USA, 2019, pp. 13–17.
[34] E. Fransson, "Driving behavior modeling and evaluation of merging control strategies-a microscopic simulation study on Sirat Expressway," 2018. [Online]. Available: https://www.diva-portal.org/smash/record.jsf?pid=diva2%3A1195623&dswid=-2880
[35] "VISSIM 2020 user manual," PTV AG, Karlsruhe, Germany, 2020. [Online]. Available: https://cgi.ptvgroup.com/visionSetups/en/filter;product=PTV%20Vissim;version=2020
[36] P. Sukennik, "Default behavioural parameter sets for AVS," PTV Group, Tech. Rep., May 2018. [Online]. Available: https://www.rupprecht-consult.eu/fileadmin/user_upload/D2.4-Vissim-extension-new-features-and-improvements_final.pdf
[37] Z. Li, H. Liu, and K. Zhang, "Sensitivity analysis of paramics based on 2K-P fractional factorial design," in *Proc. Int. Conf. Transp. Eng.* 2009, pp. 3633–3638.

HOSSAM M. ABDELGHAFFAR received the B.Sc. degree (with Hons.) in electronics engineering from the Faculty of Engineering, Mansoura University, Mansoura, Egypt, the M.Sc. degree in automatic control system engineering, Mansoura University, and the Ph.D. degree in electrical engineering, from the Bradley Department of Electrical and Computer Engineering, Virginia Tech, Blacksburg, VA, USA. He was with the Center for Sustainable Mobility with Virginia Tech Transportation Institute, Virginia Tech. He is currently an Assistant Professor with the Department of Computer Engineering and Systems, Faculty of Engineering, Mansoura University, and with the Engineering Division, New York University Abu Dhabi, Abu Dhabi, UAE. His research interests include span nonlinear dynamics and control, estimation and filtering, game theory, machine learning, connected and automated vehicles, and intelligent transport systems.

MÓNICA MENÉNDEZ (Member, IEEE) received the dual B.S. degree (*summa cum laude*) in civil and architectural engineering from the University of Miami, Coral Gables, FL, USA, in 2002, and the M.S. and Ph.D. degrees (focusing on transportation) from the University of California, Berkeley, CA, USA, in 2003 and 2006, respectively. She is currently the Associate Dean of Engineering for Graduate Programs and a Professor of civil and urban engineering with New York University Abu Dhabi (NYUAD), Abu Dhabi, UAE, and a Global Network Professor of civil and urban engineering with the Tandon School of Engineering, New York University, Brooklyn, NY, USA. She is also the Director of the NYUAD Research Center for Interacting Urban Networks (CITIES). Before joining NYUAD, she was the Director of the research group Traffic Engineering with ETH Zürich, Zürich, Switzerland, and prior to that, a Management Consultant with Bain & Company. She has authored or coauthored more than 90 journal articles and more than 200 conference contributions and technical reports in the area of transportation. Her research interests include multimodal transportation systems paying special attention to new technologies and information sources. She is an active reviewer for more than 20 journals and a member of multiple editorial boards for top journals in transportation.